

Communication

# A Novel Atypical PKC-Iota Inhibitor, Echinochrome A, Enhances Cardiomyocyte Differentiation from Mouse Embryonic Stem Cells

Hyoung Kyu Kim <sup>1,2,†</sup>, Sung Woo Cho <sup>1,3,†</sup>, Hye Jin Heo <sup>1,†</sup>, Seung Hun Jeong <sup>1</sup>, Min Kim <sup>1</sup>, Kyung Soo Ko <sup>1</sup>, Byoung Doo Rhee <sup>1</sup>, Natalia P. Mishchenko <sup>4</sup>, Elena A. Vasileva <sup>4</sup>, Sergey A. Fedoreyev <sup>4</sup>, Valentin A. Stonik <sup>4</sup> and Jin Han <sup>1,\*</sup>

<sup>1</sup> National Research Laboratory for Mitochondrial Signaling, Department of Physiology, Department of Health Sciences and Technology, BK21 Plus Project Team, Cardiovascular and Metabolic Disease Center, Inje University College of Medicine, Busan 47392, Korea; estrus74@gmail.com (H.K.K.); drswcho@hanmail.net (S.W.C.); hjheo0303@gmail.com (H.J.H.); shjeong96@gmail.com (S.H.J.); glucose1193@gmail.com (M.K.); kskomd@paik.ac.kr (K.S.K.); bdrhee@hanmail.net (B.D.R.)

<sup>2</sup> Department of Integrated Biomedical Science, Inje University College of Medicine, Busan 47392, Korea

<sup>3</sup> Division of Cardiology, Department of Internal Medicine, Inje University College of Medicine, Seoul Paik Hospital, Seoul 04551, Korea

<sup>4</sup> G.B. Elyakov Pacific Institute of Bioorganic Chemistry, Far-Eastern Branch of the Russian Academy of Science, Vladivostok 690022, Russia; mischenkonp@mail.ru (N.P.M.); vasilieva\_el\_an@mail.ru (E.A.V.); fedoreev@piboc.dvo.ru (S.A.F.); stonik@piboc.dvo.ru (V.A.S.)

\* Correspondence: phyhanj@inje.ac.kr; Tel.: +82-51-890-6727; Fax: +82-51-894-5714

† These authors contributed equally to this work.

Received: 16 May 2018; Accepted: 1 June 2018; Published: 2 June 2018



**Abstract:** Echinochrome A (EchA) is a marine bioproduct extracted from sea urchins having antioxidant, antimicrobial, anti-inflammatory, and chelating effects, and is the active component of the clinical drug histochrome. We investigated the potential use of Ech A for inducing cardiomyocyte differentiation from mouse embryonic stem cells (mESCs). We also assessed the effects of Ech A on mitochondrial mass, inner membrane potential ( $\Delta\psi_m$ ), reactive oxygen species generation, and levels of  $Ca^{2+}$ . To identify the direct target of Ech A, we performed in vitro kinase activity and surface plasmon resonance binding assays. Ech A dose-dependently enhanced cardiomyocyte differentiation with higher beating rates. Ech A (50  $\mu$ M) increased the mitochondrial mass and membrane potential but did not alter the mitochondrial superoxide and  $Ca^{2+}$  levels. The in vitro kinase activity of the atypical protein kinase C-iota (PKC $\iota$ ) was significantly decreased by 50  $\mu$ M of Ech A with an IC<sub>50</sub> for PKC $\iota$  activity of 107  $\mu$ M. Computational protein-ligand docking simulation results suggested the direct binding of Ech A to PKC $\iota$ , and surface plasmon resonance confirmed the direct binding with a low  $K_D$  of 6.3 nM. Therefore, Ech A is a potential drug for enhancing cardiomyocyte differentiation from mESCs through direct binding to PKC $\iota$  and inhibition of its activity.

**Keywords:** echinochrome A; embryonic stem cell; cardiomyocyte differentiation; PKC-iota

## 1. Introduction

Cardiovascular diseases are the leading cause of death worldwide. Significant myocardial damage can manifest as structural changes and decreased functional capacity of the heart, ultimately resulting in heart failure [1]. Unlike other human cell types, adult cardiomyocytes rarely proliferate or regenerate [2]. Therefore, many researchers have sought to develop efficient methods for cardiac regeneration after myocardial injury using cardiac stem cells [1,3,4]. However, many challenges

still remain before cardiac stem cell therapy becomes a clinically applicable strategy for cardiac regeneration [4]. Among these challenges, obtaining a large number of purified cardiomyocytes from stem cells is the most important one [2].

Pluripotent stem cells (PSCs), including embryonic stem cells and induced pluripotent stem cells, are attractive cellular sources for cardiac stem cell therapy [5]. Various chemical compounds have been studied as potential regulators of the differentiation of PSCs into cardiac lineages, and most of these chemical compounds have been related to diverse signaling pathways involving the bone morphogenetic protein, transforming growth factor, activin, nodal, Wnt, rho-associated coiled-coil kinase, and fibroblast growth factor [5,6]. However, cardiogenic molecules extracted from natural sources remain to be investigated.

Echinochrome A (Ech A) is a bioactive red pigment isolated from sea urchins [7,8]. Histochochrome, a drug form of Ech A, has shown cardioprotective effects against ischemia/reperfusion injury through its antioxidant and anti-inflammatory activities [9,10]. Our recent reports described various novel biological roles of Ech A, including enhancing mitochondria biogenesis via activation of the PGC1- $\alpha$  pathway [11], protecting mitochondrial function against cardiotoxic drugs [12], inhibiting acetylcholinesterase activity, and modulating the activity of cardiac sarcoplasmic reticulum Ca<sup>2+</sup>-ATPase [13]. Together, these previous studies suggest that Ech A is a candidate molecule to promote cardiac regeneration. In the present study, we showed the promotion of cardiomyocyte differentiation from mouse embryonic stem cells (mESCs) induced by Ech A, and the potential mechanism of Ech A-induced cardiac differentiation.

## 2. Results

### 2.1. Ech A Enhances Cardiomyocyte Differentiation from mESCs

Ech A is a water-insoluble compound extracted from the sea urchin *Scaphechinus mirabilis* and the active substance (P N002362/01) in the drug histochochrome [12]. The chemical structure of Ech A is shown in Figure 1A. Ech A treatment up to 500  $\mu$ M was not significantly toxic to EMG7 mESCs, however, Ech A reduced cell viability up to 87% of the control at a dose of 1mM (Figure 1B). For monitoring cardiomyocyte differentiation, we used EMG7 mESCs, which have a transgene consisting of cardiac-specific  $\alpha$ -myosin heavy chain ( $\alpha$ MHC) promoter-driven enhanced green fluorescent protein (GFP) [14]. Five days after the start of differentiation, 50  $\mu$ M Ech A was treated to differentiating EBs (Figure 2A). Notably, 50  $\mu$ M Ech A significantly increased the number of beating cardiomyocyte colonies in differentiating EBs, with a higher beating rate compared with the control vehicle-treated EBs (Movie 1 and Figure 2B). Ech A enhanced  $\alpha$ MHC-GFP<sup>+</sup> cardiomyocyte differentiation in a dose dependent manner, showing maximum efficacy at 50  $\mu$ M (Figure 2C). Next, we compared the mRNA expression levels of genes related to cardiomyocyte differentiation ( $\alpha$ -actinin,  $\alpha$ MHC, cTnI, cTnT, connexin 43, and MLC2) between a non-treated control, and the Ech A treated group, 7 days neonatal mice hearts and 10 weeks adult mice hearts. The mRNA level of glyceraldehyde-3-phosphate dehydrogenase (GAPDH) was used as an internal control. The mRNA expression level of marker genes in the Ech A group was similar with the neonatal and adult mice ventricle than that of the control group (Figure 2D). Interestingly, only two genes,  $\alpha$ -actinin and cTnI, showed significant different expression levels between the neonatal and adult heart. The expression of two genes in the Ech A group were more close to the neonatal heart. These results suggested that the Ech A treated differentiated cardiomyocyte-like cell is immature or neonatal, like cardiomyocyte.

By western blotting and immunocytochemistry, we found that 50  $\mu$ M Ech A also significantly increased  $\alpha$ -actinin, cTnT, and connexin 43 protein levels compared with the control (Figure 2E,F).

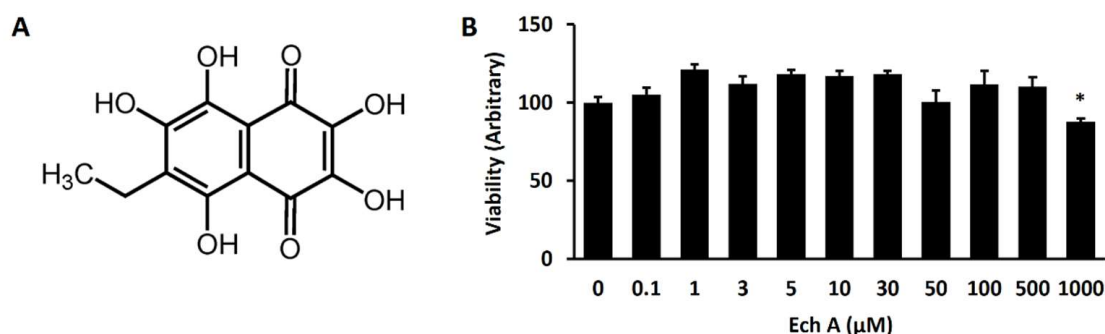


**Figure 1.** The chemical structure and cell viability effect of echinochrome A (Ech A). (A) The chemical structure of Ech A (6-ethyl-2,3,5,7,8-pentahydroxy-1,4-naphthoquinone; FW = 266.2). (B) The cell viability according to the dose of Ech A. Each group,  $n = 3-5$ .

## 2.2. Ech A Enhances Cardiomyocyte Differentiation Through Direct Binding to Atypical PKC $\iota$ and Inhibition of Its Activity

To confirm the effect of Ech A on mitochondria during cardiomyocyte differentiation, we measured the fluorescence intensity and membrane potential ( $\Delta\psi_m$ ) of the mitochondria using the Mitotracker<sup>TM</sup> Red and tetramethylrhodamine methyl ester (TMRM) fluorescent dye, respectively. Mitochondrial superoxide was measured using the MitoSox<sup>TM</sup> fluorescent dye and mitochondrial Ca<sup>2+</sup> measurements used the Rhod-2AM fluorescent dye. Ech A significantly increased the mitochondrial mass and  $\Delta\psi_m$  compared with the control, but did not affect the mitochondrial superoxide and Ca<sup>2+</sup> levels during cardiomyocyte-like cell differentiation (Figure 3A–D). Taken together, these results showed that Ech A did not alter the mitochondrial function during cardiomyocyte-like cell differentiation.

We then performed an *in vitro* kinase activity assay in differentiating EBs to identify the target of Ech A. We first performed kinase activity screening with a fixed concentration of 50  $\mu$ M to find the target kinase of Ech A (Figure 4A). The result showed the significant inhibitory effect of Ech A to atypical PKC- $\iota$  activity (PKC $\iota$ ) among the tested kinases. Since the primary screening study used a single dose treatment, the relative inhibitory value could be inaccurate. To confirm the screening result, we further performed a multi-dose half-maximal inhibitory (IC<sub>50</sub>) study of Ech A on PKC $\iota$ , which provided clear dose-dependent inhibitory effect of Ech A on PKC $\iota$ . The IC<sub>50</sub> of Ech A on PKC $\iota$  activity was 107  $\mu$ M, which was higher than primary screening result (Figure 4B).

To confirm the direct binding of Ech A and PKC $\iota$ , we performed a computational protein-ligand docking simulation and surface plasmon resonance binding assay. Computational protein-ligand docking simulation results suggested a probable binding site of Ech A to PKC $\iota$  kinase domain residues 392–402 (KEGLRPGDTTS) by polar, hydrophobic and hydrogen bond interactions (Figure 5A,B; Table 1) and the surface plasmon resonance assay confirmed the direct binding of Ech A to PKC $\iota$  with a low K<sub>D</sub> value of 6.3 nM (Figure 6).

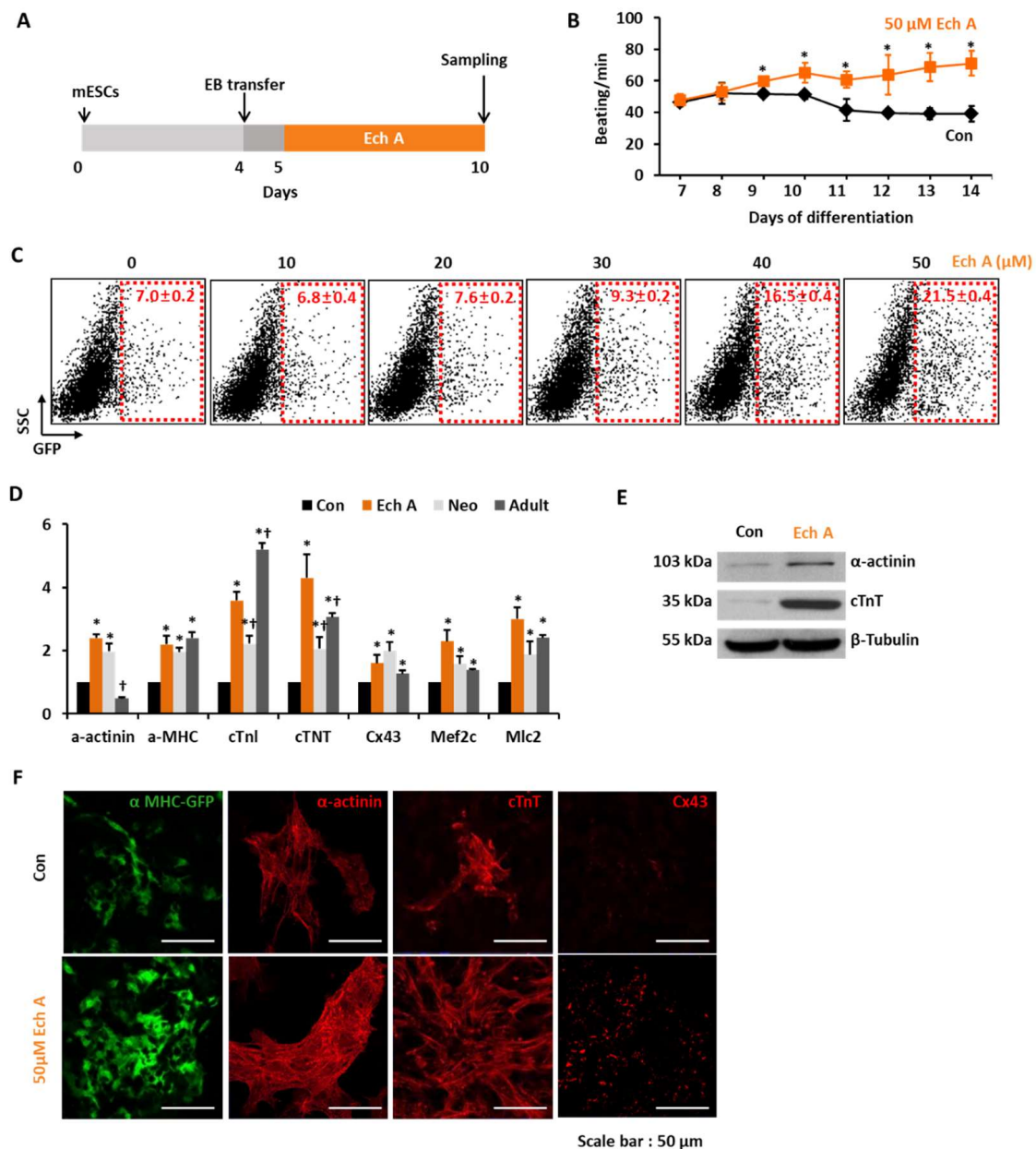


**Figure 2.** Ech A enhances cardiomyocyte differentiation from mouse embryonic stem cells (mESCs). (A) The protocol for the differentiation of cardiomyocytes from the mESCs using the hanging drop method to produce differentiated embryoid bodies (EBs). (B) The beating number per minute (BPM) of EBs during differentiation. Each group,  $n = 3$ .  $* p < 0.05$  (C) Representative FACS analyses and the percentage of mESC-derived  $\alpha$ MHC<sup>+</sup> cardiomyocyte-like cells according to the dose of Ech A. Each group,  $n = 3$ . (D) Relative mRNA expression levels of cardiomyocyte specific genes in nontreated control (Con), Ech A treatment (Ech), heart tissue from neonatal (7 day, Neo) or adult mice (10 weeks, Adult). Each group,  $n = 3$ .  $* p < 0.05$  vs. Con,  $^{\dagger} p < 0.05$  vs. Ech A. The mRNA level of glyceraldehyde-3-phosphate dehydrogenase (GAPDH) was used as an internal control. (E) Western blot analyses for the expression of cardiomyocyte specific proteins incubated with the control vehicle (Con) or 50  $\mu$ M of Ech A. (F) Images displaying  $\alpha$ MHC-GFP<sup>+</sup>,  $\alpha$ -actinin<sup>+</sup>, cTnT<sup>+</sup>, and Cx43<sup>+</sup> cells incubated with Con or 50  $\mu$ M of Ech A (scale bars, 50  $\mu$ m). SCC: side scatter cell, cTnI: cardiac troponin I, cTnT: cardiac troponin T, Cx43: connexin 43, Mef2c: Myocyte Enhancer Factor 2C, Mlc2: Myosin light chain 2.

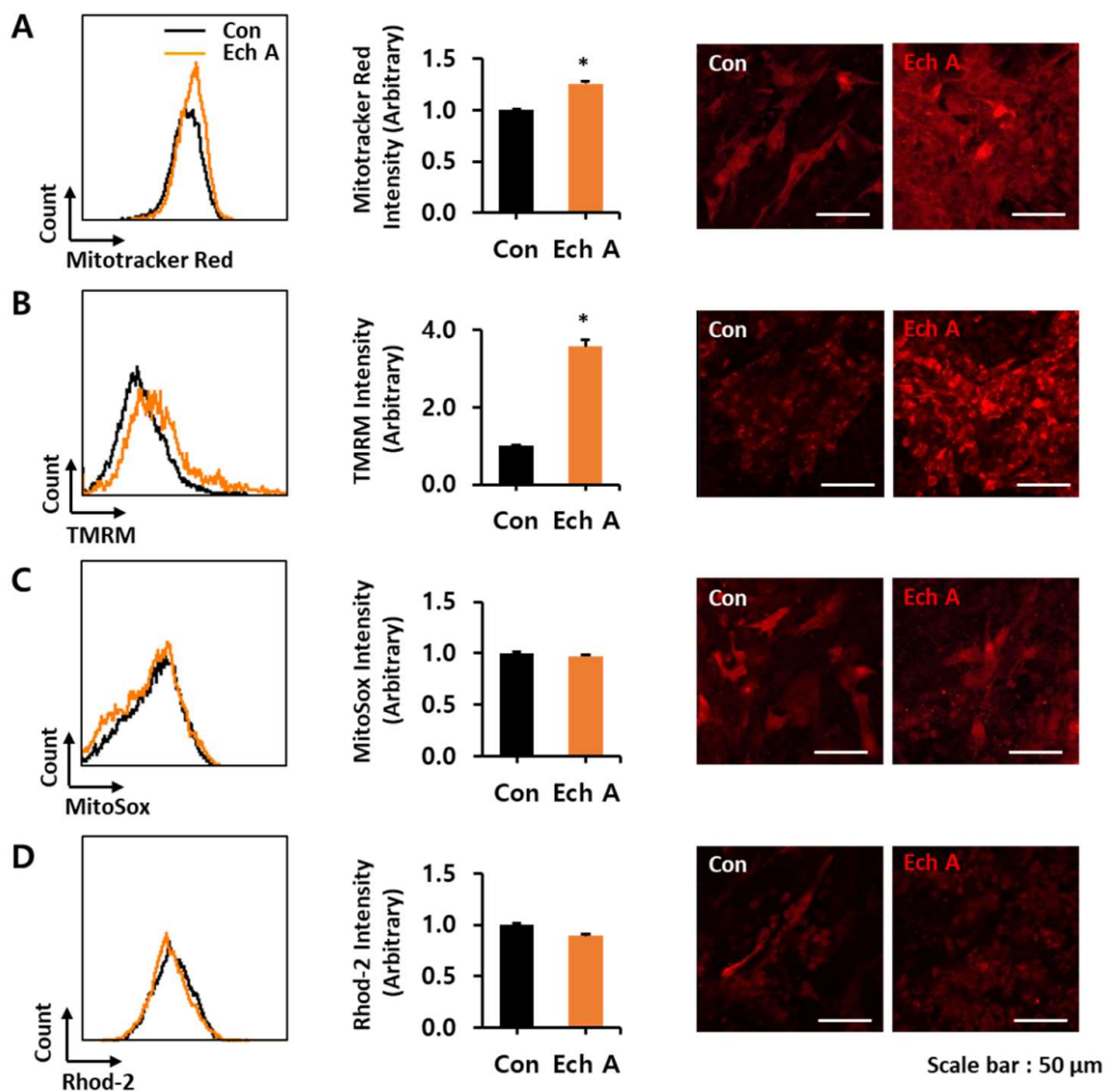


**Figure 3.** Measurement of mitochondrial functions in differentiating embryoid bodies (EBs) after Ech A treatment. Representative FACS analyses of fluorescence intensities (**left**), the percentage of relative mean fluorescence intensities (**middle**), and matched confocal microscope live cell images (**right**, scale bars, 50  $\mu$ m) of (A) Mitotracker<sup>TM</sup>, (B) mitochondria membrane potential fluorescence probe, TMRM, (C) MitoSox<sup>TM</sup>, and (D) Rhod-2, which were treated with the control vehicle (Con) or 50  $\mu$ M of Ech A. Each group,  $n = 3$ . \*  $p < 0.05$  vs non-treated control vehicle.

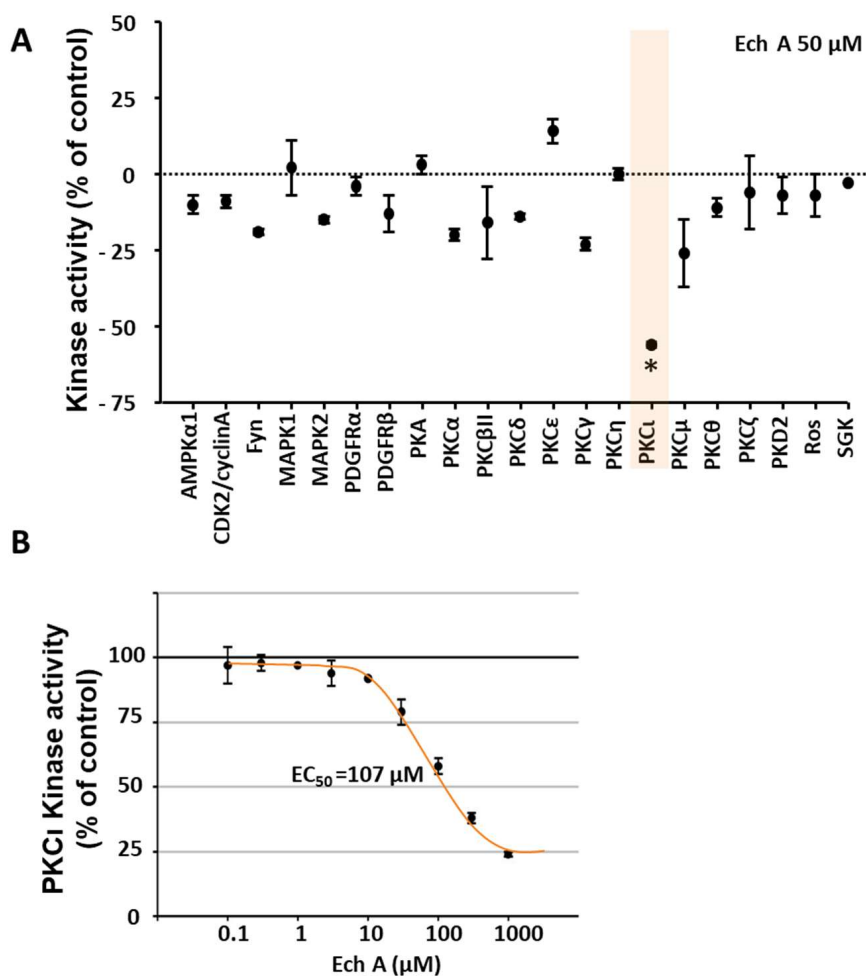


**Figure 4.** The in vitro kinase activity assay identified PKC $\iota$  as a direct target kinase of Ech A. (A) The in vitro activity assay of selected kinases in the presence of 50  $\mu$ M of Ech A. (B) The dose-dependent inhibition of PKC $\iota$  kinase activity using 0–1000  $\mu$ M of Ech A. \*  $p < 0.05$  vs vehicle control (Student's  $t$ -test) ( $n = 3$ ).

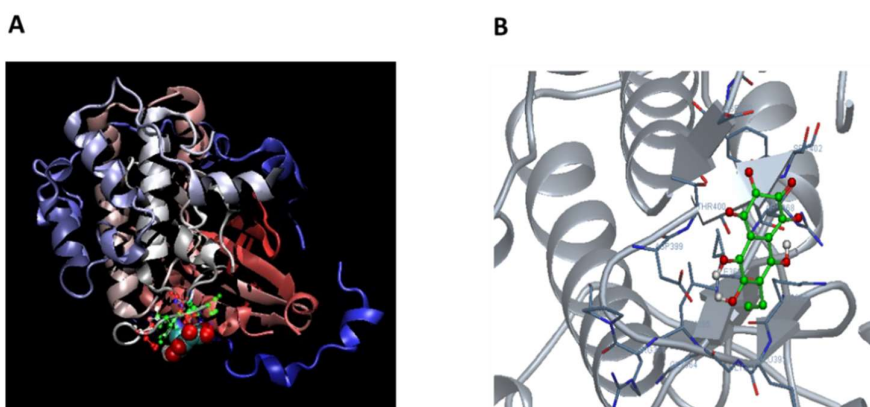


**Figure 5.** Computer simulated Ech A-PKC $\iota$  docking model. (A) A three-dimensional (3D) model of Ech A-PKC $\iota$  (PDB:3A8W) docking simulation was generated by using the online DockingServer site (<https://www.dockingserver.com>). (B) Magnified 3D structure of the Ech A-PKC $\iota$  binding site.

**Table 1.** Computer-simulated Ech A interaction residues of PKC $\iota$  kinase domain.

Residue No	Amino Acid	Interaction Type
392	LYS	Polar
395	LEU	Hydrophobic
399	ASP	Polar
400	THR	Hydrogen bonds, polar
401	THR	Hydrogen bonds, polar
402	SER	Other
420	ASP	Polar

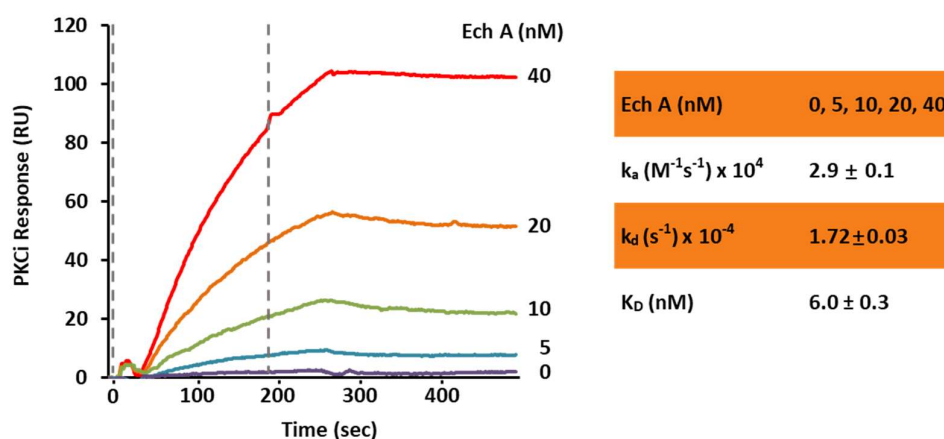


**Figure 6.** In vitro surface plasmon resonance binding assay for PKC $\iota$  and Ech A. The PKC $\iota$  binding response to Ech A was measured in the range of 0–40 nM of Ech A. The flow rate was 30  $\mu$ L/minute. The association and dissociation times were 3 min each. The calculated binding constants are shown at the bottom.  $k_a$ : Association rate,  $k_d$ : Dissociation rate,  $K_D$  (Affinity) =  $k_d/k_a$  ( $n = 3$ ).

### 3. Discussion

Various cardiogenic compounds that modulate diverse signaling pathways have been developed to induce the differentiation of cardiomyocytes from PSCs [5]; however, natural cardiogenic resources with similar action have rarely been reported. In the present study, we demonstrated the cardiogenic potential of Ech A, a natural pigment isolated from sea urchins, and elucidated its action mechanism using EBs as a model system. Previous studies reported that Histochole, a drug form of Ech A, had a cardioprotective effect involving antioxidant and anti-inflammatory mechanisms [10]. In addition, our group previously reported that Ech A had diverse biological effects involving the enhancement of mitochondrial functions [11,12]. In the present study, we firstly discovered the cardiomyogenic effect of Histochole and its novel molecular target—the PKC- $\iota$ —which may extend the application of Histochole not just as a cardioprotective drug, but for the cardiomyogenic drugs combined with stem cell therapy as well.

Ech A has no significant cytotoxicity at doses up to 500  $\mu$ M. The 50  $\mu$ M of Ech A treatment significantly enhanced the beating rate of the differentiated colony ( $71 \pm 4.5$ /min on day 14) than the untreated control ( $52 \pm 1.0$ /min on day 10). The tendency of increasing BPM is kept until 14 days in the Ech A group (Figure 2B). The heart rate of the mouse varied from 500/min to 700/min depending on the time of the day, environmental factors, and mice species. However, because of the environmental differences between the in vitro cell line and the in vivo heart condition, the heart rates of the control and Ech A treated groups were significantly different from those of the actual in vivo heart.

Mitochondrial function and signaling pathways have been investigated as a key regulator of cardiac differentiation and regeneration [15–17]. During differentiation from ESCs to cardiomyocytes, mitochondrial morphology changes dramatically, and mitochondrial biogenesis and oxidative

metabolism increase significantly [16,18]. These changes could be considered a consequence, rather than a cause, of cardiomyocyte-like cell differentiation, which simply reflect the increasing contraction and metabolic demands of cardiomyogenesis [14]. However, several studies reported that mitochondrial function and maturation does in fact play a role in controlling cardiomyocyte differentiation from PSCs [15,16]. Our group previously reported that mitochondrial pyruvate dehydrogenase phosphatase 1 regulates the early differentiation of cardiomyocytes from mESCs [19], and that a combination of cyclosporin A with antioxidants synergistically promotes cardiomyocyte differentiation from PSCs by modulating the mitochondrial permeability transition pore and redox signaling [14]. In the present study, we also investigated the effects of Ech A on mitochondria in differentiating EBs. Ech A significantly increased the mitochondrial mass and  $\Delta\psi_m$  compared to control, but did not affect mitochondrial superoxide and  $Ca^{2+}$  levels. These findings suggested that Ech A did not affect mitochondrial function in differentiating EBs, and that the increase in mitochondrial mass and  $\Delta\psi_m$  was a consequence of cardiomyocyte differentiation from EBs.

In the present study, we also showed that the cardiogenic potential of Ech A is realized via direct binding and inhibition of PKC $\iota$  activity. PKCs are serine-threonine kinases that regulate various cellular processes. These kinases are classified into the three subtypes of conventional, novel, and atypical PKCs. Several previous studies reported that some PKC subtypes regulate embryonic development and PSC self-renewal and differentiation [20–22]. Among the PKC subtypes, a recent study reported that atypical PKC $\iota$  controls stem/progenitor cell expansion via regulation of the Notch pathway [21]. Notably, knockdown of PKC $\iota$  in EBs resulted in increased expression of the cardiac-specific markers *Isl1*, *Nkx2.5*, and  $\alpha$ -actinin when compared to control EBs [21]. Similarly, our data also showed that the kinase activity of PKC $\iota$  significantly decreased in a dose-dependent manner by *in vitro* Ech A treatment. These results suggested that the inhibition of atypical PKC $\iota$  might be an important driver for cardiac differentiation of PSCs. In addition to an *in vitro* cell-free kinase activity assay, we further tested the direct binding of Ech A and PKC $\iota$  using computational modeling and a surface plasmon resonance binding assay. The docking simulations suggested direct binding of Ech A to the PKC $\iota$  kinase domain at amino acids 390–420 (Figure 5, Table 1). In the study of Pillai et al. [23], the investigators developed a novel PKC $\iota$  inhibitor ICA-1 and performed the docking site simulation between ICA-1 and PKC $\iota$  kinase domain by using PDB code 1ZRZ, similar with our present study. The ICA-1 was proposed to bind at the 469–475 amino acid residue of the PKC $\iota$  kinase domain, while Ech A is predicted to bind at the 390–420 amino acid residue of it. Both predicted sites are not located at the conserved ATP binding pocket of the PKC isoforms, suggesting the PKC $\iota$  isoform specific inhibition potential of both drugs [23]. Because PKC $\iota$  and PKC-zeta (PKC $\zeta$ ) share 84% homology in amino acid sequences in their kinase domain [23], the PKC $\iota$  specific inhibitory effect of Ech A could be supported by our kinase assay results in Figure 4A, which showed a significant difference between PKC $\iota$  and other isoforms, especially PKC $\zeta$ . However, the molecular biology based confirmation of the binding between Ech A and PKC $\iota$  kinase domain is necessary to develop the Ech A as a PKC $\iota$  inhibiting drug.

To solidify the evidence of the ligand-protein physical interaction, surface plasmon resonance showed the dose-dependent increase of the binding response signal between PKC $\iota$  and Ech A (Figure 6). The low  $K_D$  of 6.03 nM suggested a high affinity between these two components. Moreover, the Ech A-PKC $\iota$  binding did not dissociate during a 3-min time period. Interestingly, although the affinity of Ech A to PKC $\iota$  is very high, the sufficient dose for the inhibition is relatively high as  $IC_{50} = 107 \mu M$  in the cell free *in vitro* system. These affinity and efficiency should be tested more detailed in the *in vivo* system in order to develop Ech A as a PKC $\iota$  targeting drug.

Our results collectively demonstrated the effect of Ech A on cardiomyogenesis, and identified an atypical PKC $\iota$  as a direct binding target. Although the differentiated EBs and cells in the present study showed cardiomyocytes-like characteristics in the beating function and the expression of various cardiac specific markers, the *in vitro* differentiated “cardiomyocyte-like cells” still differed from real cardiomyocytes in the integrity of various ion channels, intracellular  $Ca^{2+}$  modulations, cell to cell connectivity, and so on. Therefore, further studies must elucidate (i) the regulatory mechanism of

Ech A during the enhancement of cardiomyogenesis, and (ii) the effect of Ech A on the maturation or optimization of “cardiomyocyte-like cells” to clinically applicable cardiomyocytes.

In addition to the effects on cardiomyogenesis, PKC $\iota$  inhibition has been proposed as a novel therapeutic target for acute pain syndrome [24], inflammatory disorders [25], and various cancers including prostate cancer [26], neuroblastoma [23], glioblastoma [27,28], pancreatic cancer [29], and melanoma [30]. The novel PKC $\iota$  inhibitor, Ech A, therefore has great potential for a wide range of clinical applications.

As a limitation of our study, the efficacy of Ech A is relatively lower (21% of total cell population) than established combined methods, which had improved the efficiency of stem cell differentiation to cardiomyocyte around 70–95% of the total population. According to these protocols, cardiac specification and differentiation processes are finely regulated through multiple signaling pathways involving the bone morphogenetic protein, transforming growth factor, activin, nodal, Wnt, rho-associated coiled-coil kinase, and fibroblast growth factor. Therefore, it is difficult to improve the currently saturated efficiency of cardiomyocyte differentiation by using novel molecules. Furthermore, it is hard to demonstrate the exact mechanism and interaction between novel cardiogenic molecules and other cardiogenic signaling pathways in these protocols. Indeed, recently published reports regarding cardiomyocyte differentiation from PSCs showed novel cardiogenic genes or markers, not cardiogenic molecules. In the near future, we plan to further investigate the effect of Ech A as a treatment for cardiomyocyte differentiation from human PSCs by using established high efficiency protocol.

Although adult stem cells (mesenchymal stem cells, cardiac resident stem cells, bone marrow derived stem cells, and endothelial progenitor cells) had modest effects in previous clinical trials, recent preclinical data shows there are promising when PSC-derived cardiomyocytes are implanted into infarcted primate myocardium [31]. Furthermore, implantation of cardiac cell sheets by using PSC-derived cardiomyocytes will firstly be tried in patients in the near future. Therefore, the cardiomyogenic effect of Ech A from our data is meaningful in terms of cardiac regenerative therapy by using PSC-derived cardiomyocytes that follow current trends. Therefore, the clinical importance of our study is that we firstly discovered the cardiomyogenic effect of Histochrome, a marine natural product derived drug with proven clinical safety. In addition, the finding of PKC $\iota$  as the novel molecular target of Ech A could help for the repositioning of this drug for various diseases.

## 4. Materials and Methods

### 4.1. Maintenance of mESCs

The mESC line EMG7, which has an  $\alpha$ MHC promoter-driven enhanced GFP gene, was maintained in 0.1% gelatin-coated 60-mm culture dishes without feeder layers, as previously described [14,19].

### 4.2. Induction of mESC-Derived Cardiomyocyte-Like Cell Using EBs

The hanging drop method was used to generate EBs from 750 cells in 20  $\mu$ L differentiation media (differentiation day 0, D0). On day 4 of differentiation, EBs were seeded into 1% gelatin-coated culture dishes for each experiment. During differentiation, the culture medium was changed every day. Beginning on day 6 of differentiation (2 days after plating), EB growth was monitored daily for possible self-beating activity. For analyses, EBs were dissociated with 0.1% collagenase (Worthington, Lakewood, NJ, USA) plus 0.25% trypsin-EDTA (Gibco, Seoul, Korea) for 30 min at 37 °C [19].

### 4.3. Cell Viability Assay

Cells were seeded at  $1 \times 10^4$  cells/well in 96-well tissue culture plates. Ech A was dissolved in phosphate buffered saline (PBS) and PBS was treated as a control vehicle. After 24 h of incubation, the cells were treated with 0, 0.1, 1, 3, 5, 10, 30, or 50  $\mu$ M Ech A for 24 h. Cell viability was measured using a quantitative colorimetric assay with MTT [3-(4,5-dimethylthiazol-2-yl)-2,5-diphenyltetrazolium

bromide]; (Sigma-Aldrich, Gyeonggi-do, Korea). The optical density of formazan was measured at 570 nm using a microplate reader (Molecular Devices, San Jose, CA, USA) [12].

#### 4.4. Quantitative Real-Time Polymerase Chain Reaction (PCR)

Total RNA was purified using the RNeasy mini kit (Qiagen). Complementary DNA (cDNA) was synthesized in a 50  $\mu$ L volume using Super-Script™ III First-Strand Synthesis reagents (Seoul, Korea, Invitrogen). The cDNA was amplified using *Taq*DNA polymerase (Invitrogen, Seoul, Korea) in the presence of 1  $\mu$ M oligonucleotide primers. The quantitative real-time PCR was performed using the iQ5 real-time system and the iQ SYBR™ Supermix (BioRad, Seoul, Korea). Expression of the target mRNAs relative to housekeeping gene expression (GAPDH mRNA) was calculated using the threshold cycle ( $C_T$ ) as  $r = 2^{-\Delta(\Delta C_T)}$ , where  $\Delta C_T = C_{T \text{ target}} - C_{T \text{ GAPDH}}$  and  $\Delta(\Delta C_T) = \Delta C_{T \text{ D8}} - \Delta C_{T \text{ D0}}$ . The primer sequences are shown in Table 2 [19].

**Table 2.** Quantitative real-time PCR primer sequences.

Gene	Primer Sequences
<i><math>\alpha</math>-actinin</i>	Forward 5'-AGCCAGGAACAGATGAACGA-3'
	Reverse 5'-AAGTCGATGAAGGCCTGGAA-3'
<i><math>\alpha</math>-MHC</i>	Forward 5'-GCCCAGTACCTCCGAAAGTC-3'
	Reverse 5'-GCCTTAACATACTCCTCCTTGTC-3'
<i>cTnI</i>	Forward 5'-CGTGGGAAGCAAAAGTCACCA-3'
	Reverse 5'-GTCCTCCTTCTTCACCTGCT-3'
<i>cTnT</i>	Forward 5'-CAGAGGAGGCCAACGTAGAAG-3'
	Reverse 5'-CTCCATCGGGGATCTTGGGT-3'
<i>Cx43</i>	Forward 5'-ACGGCAAGGTGAAGATGAGA-3'
	Reverse 5'-GAGAGACACCAAGGACACCA-3'
<i>Mef2c</i>	Forward 5'-ACCAGGACAAGGAATGGGAG-3'
	Reverse 5'-GGCGGCATGTTATGTAGGTG-3'
<i>MLC2</i>	Forward 5'-GGCACCAAAGAAAGCCAAGA-3'
	Reverse 5'-GGACCTGGAGCCTCTTTGAT-3'
<i>GAPDH</i>	Forward 5'-CACCATCTTCCAGGAGCGAG-3'
	Reverse 5'-CCTTCTCCATGGTGGTGAAGAC-3'

#### 4.5. Western Blot Analyses

Cells were homogenized in a protein lysis buffer and centrifuged at 10,000 $\times$  g for 10 min at 4 °C. After centrifugation, protein samples (50  $\mu$ g) were transferred to nitrocellulose membranes, which were incubated with primary antibodies against sarcomeric  $\alpha$ -actinin (Sigma-Aldrich), cTnT (Abcam, Cambridge, MA, USA), or  $\beta$ -tubulin (Abcam). Immunoreactive protein bands were detected using the SuperSignal™ West Pico system (The Thermo Scientific™, Seoul, Korea) and visualized using LAS-3000 PLUS (Fuji Photo Film Company, Tokyo, Japan) [19].

#### 4.6. Immunocytochemistry

Differentiated EBs (D8) were cultured on gelatinized 12-mm glass cover slips, fixed for 30 min at room temperature in 4% paraformaldehyde, and permeabilized for 30 min at room temperature using 0.2% Triton X-100. After permeabilization, the EBs were blocked for 10 min at room temperature with CAS-Block solution (Invitrogen), and incubated overnight at 4 °C with mouse monoclonal antibodies against sarcomeric  $\alpha$ -actinin (Abcam), cardiac troponin T (cTnT, Abcam), or connexin 43 (Cx43, Abcam). Additionally, goat anti-mouse IgG (Abcam) was used as the primary antibody to label EBs. Confocal images were obtained using a Carl Zeiss LSM 700 laser-scanning microscope (Zeiss, Oberkochen, Germany) [19].

#### 4.7. Flow Cytometry Analyses

The percentage of cardiomyocyte-like cells in differentiated EBs was analyzed using  $\alpha$ MHC-GFP. The cells were stained after dissociation of EBs with the MitoTracker™ RedCMXRos probe, TMRM, or MitoSox™ Red (Invitrogen) for 30 min at 37 °C to detect the mitochondrial membrane potential and the mitochondrial reactive oxygen species. To measure mitochondrial  $\text{Ca}^{2+}$  levels, Rhod2-AM (Invitrogen) was incubated with cells for 2 h on ice, followed by incubation for 30 min at 37 °C. After staining, the cells were washed in PBS and analyzed using a dual laser FACS Calibur instrument (Becton Dickinson, Seoul, Korea) [19].

#### 4.8. Kinase Activity Assay

A cell-free direct kinase activity assay was performed to identify the target kinases of Ech A that regulate cardiomyocyte differentiation from mESCs. The entire assay was performed using the Kinase Profiler™ Service (Eurofins Pharma Discovery Services, Aston Birmingham, UK) [32]. Individual kinase assay protocols are described in the Supplementary Materials. The dose-dependent inhibition of the PKC $\iota$  activity was determined in the presence of 0, 0.5, 1, 5, 10, 50, 100, 500, or 1000  $\mu\text{M}$  of Ech A.

#### 4.9. Computational Protein-Ligand Docking Simulation

Docking calculations were performed using DockingServer ([www.dockingserver.com](http://www.dockingserver.com)) [33]. Gasteiger partial charges were added to the ligand atoms. Nonpolar hydrogen atoms were merged, and rotatable bonds were defined. Docking calculations were performed on the human PKC $\iota$  kinase domain (PDB:3A8W) protein model. AutoDock tools were used to calculate essential hydrogen atoms, Kollman united atom type charges, and solvation parameters [34]. The van der Waals and electrostatic terms were calculated using the AutoDock parameter set- and distance-dependent dielectric functions. The Lamarckian genetic algorithm and the Solis & Wets local search method were used for docking simulations [35,36].

#### 4.10. Surface Plasmon Resonance Binding Assay

The interactions between Ech A and its direct target kinase, PKC $\iota$ , were determined using a dual channel surface plasmon resonance (SPR) instrument (SR7500DC; Reichert, Depew, NY, USA). The target full-length protein, PKC $\iota$  (Abcam), was immobilized to the sensor chip surface by free amine coupling with a mixture of 0.1 M 1-ethyl-3-(3-dimethylaminopropyl) carbodiimide hydrochloride and 0.05 M N-hydroxy succinimide injection, followed by quenching the remaining activated carboxyl groups with 1 M ethanolamine, pH 8.5. A second reference cell was treated similarly without proteins. Ech A was prepared in a running buffer (0.01% PBS-T) and injected for 3 min (association time) at a flow rate of 30  $\mu\text{L}/\text{minute}$ , followed by a dissociation phase of 3 min. Nonspecific background binding was subtracted from each sensogram using the SPR\_V4017 Data Acquisition and Alignment programs (Reichert). Binding rates and constants were independent of the flow rate over a wide range of concentrations. The best-fit kinetic parameters were obtained by global fitting analyses using Scrubber2 (Biologic Software, Canberra, Australia) [37].

#### 4.11. Statistical Analyses

Values presented are the mean  $\pm$  standard error of the mean (SEM). Data were analyzed using the one way ANOVA and unpaired Student's *t*-test. A value of  $p < 0.05$  was considered statistically significant.

## 5. Conclusions

The marine bioproduct, Ech A, is a natural molecule with a potential for enhancing cardiomyocyte differentiation from mESCs via direct binding to PKC $\iota$  and inhibition of its activity. In addition to

its known beneficial cardioprotective effects, Ech A is a promising multifaceted marine drug for the treatment of cardiovascular diseases.

**Supplementary Materials:** The following are available online at <http://www.mdpi.com/1660-3397/16/6/192/s1>. Supporting materials for protocols for kinase activity assay.

**Author Contributions:** H.K.K., S.W.C., H.J.H., S.H.J., and M.K. conducted the experiments, tests, and data analyses. N.P.M., E.A.V., S.A.F., and V.A.S. purified the echinochrome A and provided advice for the PKC $\epsilon$ -Ech A binding assay. H.K.K., S.W.C., V.A.S., and J.H. summarized the work and wrote the manuscript. K.S.K. and B.D.R. provided constructive comments for the Results and Discussion sections of the manuscript.

**Funding:** This study was supported by grants from the Priority Research Centers Program, Basic Science Research Program, and International Research & Development Program through the National Research Foundation of Korea (NRF), funded by the Ministry of Education, Science, and Technology (2010-0020224, 2015R1A2A1A13001900, 2015R1D1A1A01057937, and 2017K1A3A1A49070056). The study was carried out under support of the Ministry of Education and Science of the Russian Federation (RFMEFI61317X0076) using the equipment of the Collective Facilities Center (The Far Eastern Center for Structural Molecular Research (NMR/MS) PIBOC FEB RAS).

**Conflicts of Interest:** The authors declare no conflict of interest.

## References

- Hansson, E.M.; Lindsay, M.E.; Chien, K.R. Regeneration next: Toward heart stem cell therapeutics. *Cell Stem Cell* **2009**, *5*, 364–377. [[CrossRef](#)] [[PubMed](#)]
- Lin, Z.; Pu, W.T. Strategies for cardiac regeneration and repair. *Sci. Transl. Med.* **2014**, *6*, 239rv1. [[CrossRef](#)] [[PubMed](#)]
- Passier, R.; van Laake, L.W.; Mummery, C.L. Stem-cell-based therapy and lessons from the heart. *Nature* **2008**, *453*, 322–329. [[CrossRef](#)] [[PubMed](#)]
- Segers, V.F.; Lee, R.T. Stem-cell therapy for cardiac disease. *Nature* **2008**, *451*, 937–942. [[CrossRef](#)] [[PubMed](#)]
- Burridge, P.W.; Keller, G.; Gold, J.D.; Wu, J.C. Production of de novo cardiomyocytes: Human pluripotent stem cell differentiation and direct reprogramming. *Cell Stem Cell* **2012**, *10*, 16–28. [[CrossRef](#)] [[PubMed](#)]
- Hong, S.P.; Song, S.; Cho, S.W.; Lee, S.; Koh, B.I.; Bae, H.; Kim, K.H.; Park, J.S.; Do, H.S.; Im, I.; et al. Generation of PDGFR $\alpha$ + Cardioblasts from Pluripotent Stem Cells. *Sci. Rep.* **2017**, *7*, 41840. [[CrossRef](#)] [[PubMed](#)]
- Lebedev, A.V.; Ivanova, M.V.; Levitsky, D.O. Echinochrome, a naturally occurring iron chelator and free radical scavenger in artificial and natural membrane systems. *Life Sci.* **2005**, *76*, 863–875. [[CrossRef](#)] [[PubMed](#)]
- Thomson, R.H. Distribution of naturally occurring quinones. *Pharm. Weekbl. Sci.* **1991**, *13*, 70–73. [[CrossRef](#)] [[PubMed](#)]
- Shvilkin, A.V.; Serebriakov, L.I.; Tskitishvili, O.V.; Sadretdinov, S.M.; Kol'tsova, E.A.; Maksimov, O.B.; Mishchenko, N.P.; Novikov, V.L.; Levitskii, D.O.; Ruda, M. Effect of echinochrome on experimental myocardial reperfusion injury. *Kardiologiya* **1991**, *31*, 79–81. [[PubMed](#)]
- Buimov, G.A.; Maksimov, I.V.; Perchatkin, V.A.; Repin, A.N.; Afanas'ev, S.A.; Markov, V.A.; Karpov, R.S. Effect of the bioantioxidant histochrome on myocardial injury in reperfusion therapy on patients with myocardial infarction. *Terapevticheskii Arkhiv* **2002**, *74*, 12–16. [[PubMed](#)]
- Jeong, S.H.; Kim, H.K.; Song, I.S.; Noh, S.J.; Marquez, J.; Ko, K.S.; Rhee, B.D.; Kim, N.; Mishchenko, N.P.; Fedoreyev, S.A.; et al. Echinochrome increases mitochondrial mass and function by modulating mitochondrial biogenesis regulatory genes. *Mar. Drugs* **2014**, *12*, 4602–4615. [[CrossRef](#)] [[PubMed](#)]
- Jeong, S.H.; Kim, H.K.; Song, I.S.; Lee, S.J.; Ko, K.S.; Rhee, B.D.; Kim, N.; Mishchenko, N.P.; Fedoreyev, S.A.; Stonik, V.A.; et al. Echinochrome A protects mitochondrial function in cardiomyocytes against cardiotoxic drugs. *Mar. Drugs* **2014**, *12*, 2922–2936. [[CrossRef](#)] [[PubMed](#)]
- Kim, H.K.; Youm, J.B.; Jeong, S.H.; Lee, S.R.; Song, I.S.; Ko, T.H.; Pronto, J.R.; Ko, K.S.; Rhee, B.D.; Kim, N.; et al. Echinochrome A regulates phosphorylation of phospholamban Ser16 and Thr17 suppressing cardiac SERCA2A Ca<sup>2+</sup>(+) reuptake. *Pflugers Arch.* **2015**, *467*, 2151–2163. [[CrossRef](#)] [[PubMed](#)]
- Cho, S.W.; Park, J.S.; Heo, H.J.; Park, S.W.; Song, S.; Kim, I.; Han, Y.M.; Yamashita, J.K.; Youm, J.B.; Han, J.; et al. Dual modulation of the mitochondrial permeability transition pore and redox signaling synergistically promotes cardiomyocyte differentiation from pluripotent stem cells. *J. Am. Heart Assoc.* **2014**, *3*, e000693. [[CrossRef](#)] [[PubMed](#)]

15. Spitkovsky, D.; Sasse, P.; Kolossov, E.; Bottinger, C.; Fleischmann, B.K.; Hescheler, J.; Wiesner, R.J. Activity of complex III of the mitochondrial electron transport chain is essential for early heart muscle cell differentiation. *FASEB J.* **2004**, *18*, 1300–1302. [[CrossRef](#)] [[PubMed](#)]
16. Chung, S.; Dzeja, P.P.; Faustino, R.S.; Perez-Terzic, C.; Behfar, A.; Terzic, A. Mitochondrial oxidative metabolism is required for the cardiac differentiation of stem cells. *Nat. Clin. Pract. Cardiovasc. Med.* **2007**, *4* (Suppl. 1), S60–S67. [[CrossRef](#)] [[PubMed](#)]
17. Porter, G.A., Jr.; Hom, J.; Hoffman, D.; Quintanilla, R.; de Mesy Bentley, K.; Sheu, S.S. Bioenergetics, mitochondria, and cardiac myocyte differentiation. *Prog. Pediatr. Cardiol.* **2011**, *31*, 75–81. [[CrossRef](#)] [[PubMed](#)]
18. Tohyama, S.; Hattori, F.; Sano, M.; Hishiki, T.; Nagahata, Y.; Matsuura, T.; Hashimoto, H.; Suzuki, T.; Yamashita, H.; Satoh, Y.; et al. Distinct metabolic flow enables large-scale purification of mouse and human pluripotent stem cell-derived cardiomyocytes. *Cell Stem Cell* **2013**, *12*, 127–137. [[CrossRef](#)] [[PubMed](#)]
19. Heo, H.J.; Kim, H.K.; Youm, J.B.; Cho, S.W.; Song, I.S.; Lee, S.Y.; Ko, T.H.; Kim, N.; Ko, K.S.; Rhee, B.D.; et al. Mitochondrial pyruvate dehydrogenase phosphatase 1 regulates the early differentiation of cardiomyocytes from mouse embryonic stem cells. *Exp. Mol. Med.* **2016**, *48*, e254. [[CrossRef](#)] [[PubMed](#)]
20. Mahato, B.; Home, P.; Rajendran, G.; Paul, A.; Saha, B.; Ganguly, A.; Ray, S.; Roy, N.; Swerdlow, R.H.; Paul, S. Regulation of mitochondrial function and cellular energy metabolism by protein kinase C-lambda/iota: A novel mode of balancing pluripotency. *Stem Cells* **2014**, *32*, 2880–2892. [[CrossRef](#)] [[PubMed](#)]
21. Mah, I.K.; Soloff, R.; Hedrick, S.M.; Mariani, F.V. Atypical PKC-iota Controls Stem Cell Expansion via Regulation of the Notch Pathway. *Stem Cell Rep.* **2015**, *5*, 866–880. [[CrossRef](#)] [[PubMed](#)]
22. Seidl, S.; Braun, U.; Roos, N.; Li, S.; Ludtke, T.H.; Kispert, A.; Leitges, M. Phenotypical analysis of atypical PKCs in vivo function display a compensatory system at mouse embryonic day 7.5. *PLoS ONE* **2013**, *8*, e62756. [[CrossRef](#)] [[PubMed](#)]
23. Pillai, P.; Desai, S.; Patel, R.; Sajan, M.; Farese, R.; Ostrov, D.; Acevedo-Duncan, M. A novel PKC-iota inhibitor abrogates cell proliferation and induces apoptosis in neuroblastoma. *Int. J. Biochem. Cell Biol.* **2011**, *43*, 784–794. [[CrossRef](#)] [[PubMed](#)]
24. Jatoi, A.; Grudem, M.E.; Dockter, T.J.; Block, M.S.; Villasboas, J.C.; Tan, A.; Deering, E.; Kasi, P.M.; Mansfield, A.S.; Botero, J.P.; et al. A proof-of-concept trial of protein kinase C iota inhibition with auranofin for the paclitaxel-induced acute pain syndrome. *Support. Care Cancer* **2017**, *25*, 833–838. [[CrossRef](#)] [[PubMed](#)]
25. Chand, S.; Mehta, N.; Bahia, M.S.; Dixit, A.; Silakari, O. Protein kinase C-theta inhibitors: A novel therapy for inflammatory disorders. *Curr. Pharm. Des.* **2012**, *18*, 4725–4746. [[CrossRef](#)] [[PubMed](#)]
26. Win, H.Y.; Acevedo-Duncan, M. Role of protein kinase C-iota in transformed non-malignant RWPE-1 cells and androgen-independent prostate carcinoma DU-145 cells. *Cell Prolif.* **2009**, *42*, 182–194. [[CrossRef](#)] [[PubMed](#)]
27. Desai, S.R.; Pillai, P.P.; Patel, R.S.; McCray, A.N.; Win-Piazza, H.Y.; Acevedo-Duncan, M.E. Regulation of Cdk7 activity through a phosphatidylinositol (3)-kinase/PKC-iota-mediated signaling cascade in glioblastoma. *Carcinogenesis* **2012**, *33*, 10–19. [[CrossRef](#)] [[PubMed](#)]
28. McCray, A.N.; Desai, S.; Acevedo-Duncan, M. The interruption of PKC-iota signaling and TRAIL combination therapy against glioblastoma cells. *Neurochem. Res.* **2014**, *39*, 1691–1701. [[CrossRef](#)] [[PubMed](#)]
29. Butler, A.M.; Scotti Buzhardt, M.L.; Erdogan, E.; Li, S.; Inman, K.S.; Fields, A.P.; Murray, N.R. A small molecule inhibitor of atypical protein kinase C signaling inhibits pancreatic cancer cell transformed growth and invasion. *Oncotarget* **2015**, *6*, 15297–15310. [[CrossRef](#)] [[PubMed](#)]
30. Ratnayake, W.S.; Apostolatos, A.H.; Ostrov, D.A.; Acevedo-Duncan, M. Two novel atypical PKC inhibitors; ACPD and DNDA effectively mitigate cell proliferation and epithelial to mesenchymal transition of metastatic melanoma while inducing apoptosis. *Int. J. Oncol.* **2017**, *51*, 1370–1382. [[CrossRef](#)] [[PubMed](#)]
31. Shiba, Y.; Gomibuchi, T.; Seto, T.; Wada, Y.; Ichimura, H.; Tanaka, Y.; Ogasawara, T.; Okada, K.; Shiba, N.; Sakamoto, K.; et al. Allogeneic transplantation of iPS cell-derived cardiomyocytes regenerates primate hearts. *Nature* **2016**, *538*, 388–391. [[CrossRef](#)] [[PubMed](#)]
32. Maculins, T.; Carter, N.; Dorval, T.; Hudson, K.; Nissink, J.W.; Hay, R.T.; Alwan, H. A Generic Platform for Cellular Screening Against Ubiquitin Ligases. *Sci. Rep.* **2016**, *6*, 18940. [[CrossRef](#)] [[PubMed](#)]
33. Bikadi, Z.; Hazai, E. Application of the PM6 semi-empirical method to modeling proteins enhances docking accuracy of AutoDock. *J. Cheminform.* **2009**, *1*, 15. [[CrossRef](#)] [[PubMed](#)]

34. Morris, G.M.; Goodsell, D.S.; Halliday, R.S.; Huey, R.; Hart, W.E.; Belew, R.K.; Olson, A.J. Automated docking using a Lamarckian genetic algorithm and an empirical binding free energy function. *J. Comput. Chem.* **1998**, *19*, 1639–1662. [[CrossRef](#)]
35. Solis, F.J.; Wets, R.J.-B. Minimization by Random Search Techniques. *Math. Oper. Res.* **1981**, *6*, 19–30. [[CrossRef](#)]
36. Ali, A.G.; Mohamed, M.F.; Abdelhamid, A.O.; Mohamed, M.S. A novel adamantane thiazole derivative induces mitochondria-mediated apoptosis in lung carcinoma cell line. *Bioorg. Med. Chem.* **2017**, *25*, 241–253. [[CrossRef](#)] [[PubMed](#)]
37. Serasinghe, M.N.; Seneviratne, A.M.; Smrcka, A.V.; Yoon, Y. Identification and characterization of unique proline-rich peptides binding to the mitochondrial fission protein hFis1. *J. Biol. Chem.* **2010**, *285*, 620–630. [[CrossRef](#)] [[PubMed](#)]



© 2018 by the authors. Licensee MDPI, Basel, Switzerland. This article is an open access article distributed under the terms and conditions of the Creative Commons Attribution (CC BY) license (<http://creativecommons.org/licenses/by/4.0/>).